

**Rate of Adsorption of Methanol at a Polycrystalline Pt
Electrode**

by Sol Gilman

ARL-TR-6570

August 2013

NOTICES

Disclaimers

The findings in this report are not to be construed as an official Department of the Army position unless so designated by other authorized documents.

Citation of manufacturer's or trade names does not constitute an official endorsement or approval of the use thereof.

Destroy this report when it is no longer needed. Do not return it to the originator.

Army Research Laboratory

Adelphi, MD 20783-1197

ARL-TR-6570

August 2013

Rate of Adsorption of Methanol at a Polycrystalline Pt Electrode

Sol Gilman

Sensors and Electron Devices Directorate, ARL

REPORT DOCUMENTATION PAGE			Form Approved OMB No. 0704-0188		
Public reporting burden for this collection of information is estimated to average 1 hour per response, including the time for reviewing instructions, searching existing data sources, gathering and maintaining the data needed, and completing and reviewing the collection information. Send comments regarding this burden estimate or any other aspect of this collection of information, including suggestions for reducing the burden, to Department of Defense, Washington Headquarters Services, Directorate for Information Operations and Reports (0704-0188), 1215 Jefferson Davis Highway, Suite 1204, Arlington, VA 22202-4302. Respondents should be aware that notwithstanding any other provision of law, no person shall be subject to any penalty for failing to comply with a collection of information if it does not display a currently valid OMB control number. PLEASE DO NOT RETURN YOUR FORM TO THE ABOVE ADDRESS.					
1. REPORT DATE (DD-MM-YYYY) August 2013		2. REPORT TYPE Final		3. DATES COVERED (From - To)	
4. TITLE AND SUBTITLE Rate of Adsorption of Methanol at a Polycrystalline Pt Electrode			5a. CONTRACT NUMBER		
			5b. GRANT NUMBER		
			5c. PROGRAM ELEMENT NUMBER		
6. AUTHOR(S) Sol Gilman			5d. PROJECT NUMBER		
			5e. TASK NUMBER		
			5f. WORK UNIT NUMBER		
7. PERFORMING ORGANIZATION NAME(S) AND ADDRESS(ES) U.S. Army Research Laboratory ATTN: RDRL-SED-C 2800 Powder Mill Road Adelphi, MDS 20783-1197			8. PERFORMING ORGANIZATION REPORT NUMBER ARL-TR-6570		
9. SPONSORING/MONITORING AGENCY NAME(S) AND ADDRESS(ES)			10. SPONSOR/MONITOR'S ACRONYM(S)		
			11. SPONSOR/MONITOR'S REPORT NUMBER(S)		
12. DISTRIBUTION/AVAILABILITY STATEMENT Approved for public release; distribution unlimited.					
13. SUPPLEMENTARY NOTES					
14. ABSTRACT Methanol continues to be the most likely practical fuel for fuel cells operating at low internal temperatures. Enhanced knowledge of the electrochemistry of the anodic oxidation of methanol at platinum electrodes could assist in the attempts to improve the platinum-based electrocatalysts that are commonly employed in that technology. Numerous studies of the overall kinetics of the methanol anode have included identifying dissolved products and adsorbed species but little has been reported on the quantitative rate of the adsorption process. In the lower range of potentials, where no oxidative products are released to the electrolyte, the adsorption is initiated by an electrochemical dehydrogenation and follows Elovich kinetics. Specifically, adsorbed anions affect both the rate of methanol adsorption and its oxidation to desorbed products.					
15. SUBJECT TERMS methanol anode, methanol fuel cell, adsorption of methanol, anion adsorption					
16. SECURITY CLASSIFICATION OF:			17. LIMITATION OF ABSTRACT UU	18. NUMBER OF PAGES 32	19a. NAME OF RESPONSIBLE PERSON Sol Gilman
a. REPORT Unclassified	b. ABSTRACT Unclassified	c. THIS PAGE Unclassified			19b. TELEPHONE NUMBER (Include area code) (301) 394-0339

Contents

List of Figures	iv
Summary	1
1. Introduction	3
2. Experimental	4
2.1 Supplies and Equipment.....	4
2.2 Electrodes	4
2.3 Electrode Pre-Treatment.....	5
3. Results and Discussion	5
3.1 Polarization Curve for Methanol Oxidation.....	5
3.2 Anodic Charge by Chronocoulometry	6
3.3 Anodic Charge by Linear Anodic Scan.....	8
3.4 Measurement of Fractional Surface Coverage by Hydrogen Underpotential Deposition	8
3.5 Comparison of Q_a with Q_a'	9
3.6 Comparison of Q_a' with ΔQ_H	10
3.7 Kinetics of Methanol Adsorption Measured by Hydrogen Blocking.....	12
3.8 Dependence of Adsorption Rate on Methanol Concentration.....	14
3.9 Dependence of Adsorption Rate on Electrode Potential	15
3.10 “Poisoning Effect” of Adsorbed Methanol	17
3.11 Effect of Adsorbed Anions on the Adsorption and Oxidation of Methanol	19
4. Conclusion	21
5. References	23
Distribution List	25

List of Figures

Figure 1. CV scan for methanol oxidation at a Pt electrode in 1 M HClO ₄ containing 0.005 M methanol. The electrode was pre-treated and then reduced at 0.06 V before scanning at 5 mV/sec.	6
Figure 2. Values of charge corresponding to methanol adsorption: (a) at 0.4 V from a 0.001 M solution and (b) at 0.3 V from a 0.005 M solution of methanol. Q_a = charge measured during adsorption. Q_a' = charge measured during linear anodic scan of adlayer. Θ_H = fractional surface coverage based on the hydrogen underpotential deposition (UPD).	7
Figure 3. Representative anodic CV scans at 200 V/s for tracking (by oxidation) the adsorption of methanol at 0.4 V from a 0.001 M solution of methanol in a 1 M HClO ₄ supporting electrolyte.....	8
Figure 4. Representative cathodic CV scans at 200 V/s for tracking (by hydrogen UPD) the adsorption of methanol from a 0.001 M solution of methanol in a 1 M HClO ₄ supporting electrolyte.....	9
Figure 5. Values of charge corresponding to oxidation of the methanolic adlayer and blocking of hydrogen adsorption sites at (a) 0.4 V, 0.001 M methanol and (b) 0.3 V, 0.005 M methanol.	11
Figure 6. Fractional surface coverage of electrode with methanol as determined by hydrogen blocking. Methanol adsorbed from (a) a 0.001 M solution of methanol and (b) a 0.005 M solution of methanol.	13
Figure 7. Dependence of adsorption rate on methanol concentration. Adsorption rates were measured at 0.4 V and a fractional surface coverage of 0.5.	15
Figure 8. Potential dependence of the methanol adsorption rate.	16
Figure 9. Fractional surface coverage of methanol-free electrode with hydrogen.	17
Figure 10. Partial currents at 0.6 V.	18
Figure 11. Dependence of oxidation/desorption current on methanolic surface coverage.....	19
Figure 12. Effect of specifically adsorbed anions on anodic oxidation of methanol.....	20
Figure 13. Effect of specifically adsorbed anions on the methanol adsorption rate.	21

Summary

Prior research on methanol adsorption/oxidation at the platinum/acid interface has concluded that the adsorption process is oxidative, resulting in a number of surface species with various stoichiometries and attachments to the surface. The methanolic surface species do not further oxidize and desorb at potentials lower than ~ 0.5 V. One or more of those species can act as intermediates or poisons in the further oxidation to desorbed products, depending on the potential. The relative amounts of the various surface species has not yet been determined by spectroscopy and attempts to do so using coulometry are hampered by the multiple possibilities for surface bonding. However, some characterization is possible with respect to ratio of electrons for adsorption for further oxidation and the ratio of electrons for either of the latter processes to hydrogen adsorption sites. The values found in this study, >1 , agree generally with those reported by other investigators.

In spite of the complexity of the adlayer, it was possible to monitor the rate of the oxidation/adsorption process and produce results with good regularity when the adsorption was measured based on hydrogen blocking. For the range of potentials from 0.2 to 0.5 V versus the reversible hydrogen electrode (RHE), where oxidation of methanol leads only to adsorption, the Elovich equation applies very well for surface coverages $>\sim 0.1$ and just before reaching plateau levels. As expected, rates of adsorption vary linearly with the concentration of the methanol solution when compared to a constant surface concentration. Rates of adsorption reported by other investigators in a sulfuric acid supporting electrolyte are ~ 2 orders of magnitude slower than those reported here, likely due to the effect of specific adsorption of bisulfate ions. Not previously reported is the observation that the rate of adsorption below 0.5 V follows a Tafel relationship down to a potential of ~ 0.2 V at a fixed coverage of the surface with the methanolic adsorbate, suggesting that the oxidation/adsorption process is electrochemical rather than chemical in nature and not a function of surface coverage with hydrogen atoms. Steric effects of adsorbed hydrogen may be responsible for lower rates of adsorption at potentials of 0.1 V and below. A Tafel plot provides an apparent value of $\alpha n = 0.8$. This could be tentatively interpreted as corresponding to a 2-electron oxidation of methanol to a CHOH surface species with transference number of 0.4.

A potential of 0.6 V was chosen to examine the effect of methanol on the current, (I_{ox}), which results in oxidation of methanol to the final desorbed products (reportedly, carbon dioxide, formic acid, and formaldehyde). After correcting for the current corresponding to adsorption only, the "turnover current," I_{ox} , was found to decline linearly with an increase of Θ_M . This seems surprising at first considering that the rate of adsorption decreases exponentially with the increase of Θ_M reflecting surface inhomogeneity and the occupancy with adsorbed intermediates

at the sites with the highest heats of adsorption. This may imply that once adsorbed, the active intermediate has relatively high mobility and good distribution on available surface sites.

Adsorbed chloride ions drastically reduce the rate of adsorption of methanol and the anodic current corresponding to oxidation of methanol to final products, suggesting that both processes involve the same dehydrogenation step. Adsorbed bisulfate ions have a moderate effect on the initial rate of methanol adsorption, paralleling the observation that the anodic current is only moderately affected.

1. Introduction

After many decades of research and development, ambient temperature methanol fuel cells are emerging as a practical technology. However, fundamental improvements in the basic components still limit wide-spread application of this power source. The present anodic electrocatalyst is platinum (Pt)-based in an acid environment and the search for improvement in the performance, reliability and cost of that component has been the chief motivation for research in the area of adsorption/reaction mechanisms that has continued from the early 1960s to the present day. Past results are summarized in several reviews (1–3) and many journal articles, of which only a sampling are referenced in this report.

The study of methanol adsorption on Pt electrodes has involved using a variety of approaches including various voltammetric techniques (1–14), radioisotope-tagged methanol and anions (15–17), in-situ infrared spectroscopy and electron microscopy (18–24), online and in-situ mass spectrometry (13, 26–28), and oriented single crystals (23, 25, 29). All of the results to date point to a very complicated series of reactions that lead to the release of a number of final products of reaction. The present qualitative understanding of the situation in acid electrolytes at near ambient temperatures can be summarized as follows:

1. Starting with a bare surface and proceeding up the voltage scale from 0 V and below ~ 0.5 V versus the RHE, the currents that flow result in the accumulation of surface species with no release of oxidation products (i.e., no “turnover” current) to the external electrolyte as suggested by voltammetry and confirmed by in-situ mass spectrometry.
2. As suggested by the voltammetric results and confirmed by the more recent in-situ analytical investigations (18, 19, 24, 25), the adlayer is comprised of a number of species resulting from the partial dehydrogenation of methanol including CH_2OH , CHOH , and CHO that are bonded to one, two, and three Pt surface sites, respectively; and CO in the one-site (linear or atop), two-site (bridged); and three-site configuration. The predominance of any of these adsorbed species depends on the specific experimental conditions (e.g., potential, surface preparation, crystal orientation, and temperature).
3. The final products of methanol oxidation include formaldehyde, formic acid, methyl formate, and carbon dioxide (CO_2) (26, 27) resulting from the oxidative combination of one or more of the adsorbed species with water or hydroxyl ions. The entire oxidative process may involve desorption and readsorption/further oxidation of dissolved products other than CO_2 . Adsorbed CO is the most refractory of the surface species and is often considered to act as a “poison” to the production of the final products. However, at sufficiently high potentials, the oxidation of adsorbed CO must also contribute to the total anodic current and may indeed be the chief intermediate in any extent of CO_2 production.

By the same token, any of the other more refractory adsorbed species may act as a “poison” at lower potentials.

Measurements of methanol adsorption rates have been reported previously (4, 5, 14, 16, 27). These have been largely fragmentary in any one particular study (e.g., single potential, different acids, and different concentrations and surface preparation) and have been largely performed in a sulfuric acid supporting electrolyte with results reflecting some competition with the bisulfate anion, as shown in some of the referenced radioisotopic studies. The purpose of this study is to reinvestigate the rate of initial formation of the methanolic adlayer in a perchloric acid (HClO_4) electrolyte that is generally viewed as presenting very low anion adsorption. Some exploration of the effect of sulfate and chloride additions to the electrolyte was also conducted in this study.

2. Experimental

2.1 Supplies and Equipment

All measurements were made at room temperature (21 °C) in a 1 M solution of HClO_4 with various additions of Sigma-Aldrich spectrophotometric-grade methanol and reagent-grade hydrochloric or sulfuric acids. The test vessel was fabricated of Pyrex glass containing two platinized Pt counter electrodes isolated from the main compartment by glass frits. The acid solution was prepared using “Millipore” water with a resistivity of 18.2 $\text{M}\Omega\text{-cm}$ and redistilled HClO_4 (Sigma–Aldrich). Solutions were de-aerated with reagent grade argon for several hours. Electrochemical measurements were made using a Gamry Reference 3000 potentiostat.

2.2 Electrodes

The working electrode was a commercially pure (CP) grade Pt wire of 0.08 cm diameter. The wire was etched lightly in aqua regia, flame annealed, encased in shrinkable polytetrafluoroethylene (PTFE) tubing to expose a 1 cm length with a geometric area of 0.26 cm^2 and then lightly etched again. The working electrode was periodically immersed in hot chromic acid cleaning solution to remove particularly refractory surface contamination. Based on cathodic hydrogen deposition as previously described (31) and the assumption of 210 microcoulombs/ cm^2 for a smooth Pt surface, this electrode had a hydrogen capacity, $^sQ_{\text{H}}$, of 107 microcoulombs, a roughness factor of 2.0 and a “hydrogen area,” A_{H} , of 0.52 cm^2 . All quantities expressed on a per cm^2 basis below use the latter value of A_{H} . The value of $^sQ_{\text{H}}$ remained constant during several months of experimentation with the electrode.

The two counter electrodes were platinized Pt foils of 1 cm^2 geometric area each. The use of a Pd/H electrode as reference allowed very close placement parallel to the working electrode. It was prepared as described previously (31). The Pd/H electrode was re-hydrogenated after several days of use and its potential was monitored against a saturated calomel electrode (SCE) in a

separate vessel every few hours. Between re-hydrogenations, the electrode was found to maintain a potential of ~ 0.02 V within a few millivolts versus the RHE. All potentials applied and reported here were adjusted to that of a RHE.

2.3 Electrode Pre-Treatment

The general approach of using a staircase of pulses was used to condition the electrode and prepare the surrounding electrolyte for controlled mass transport was described previously (31). The following pretreatment was found to result in an extremely reproducible electrode reference state as judged by the response to cathodic and anodic scans performed in the supporting electrolyte. By that measure, a clean surface could be maintained for upwards of 1000 s when methanol was not present:

1. 0 V for 1 s to desorb anions (with argon flow)
 2. 1.8 V for 2 s to remove oxidizable organics (with argon flow)
 3. 1.2 V for 30 s (with argon flow) to retain the oxidized surface that prevents adsorption of organic impurities while sweeping oxygen away.
 4. 1.2 V for 60 s (no argon) to continue to retain the oxidized surface while allowing the electrolyte to become quiescent.
 5. Potential step in the range 0.06 to 0.6 V for duration, t seconds to reduce the electrode surface and to permit adsorption of methanol before applying a measurement scan or pulse.
-

3. Results and Discussion

3.1 Polarization Curve for Methanol Oxidation

A cyclic voltammetry (CV) scan for methanol appears in figure 1. At this slow sweep speed, the anodic currents reflect “turnover” (rather than adsorptive) processes that release products of oxidation to the electrolyte. Two aspects of the figure are particularly relevant to the present study of adsorption:

1. Moving in the anodic direction, there is no significant current corresponding to product release to the electrolyte below 0.4 V, as could be expected from the reported results of online mass spectrometry (12). Therefore, oxidative currents measured at the lower potentials correspond to adsorption.
2. Moving in the cathodic direction from high anodic potentials, no significant current is observed above ~ 0.9 V. The electrode’s passivity under those circumstances was used in designing the pre-treatment sequence described in section 2.3.

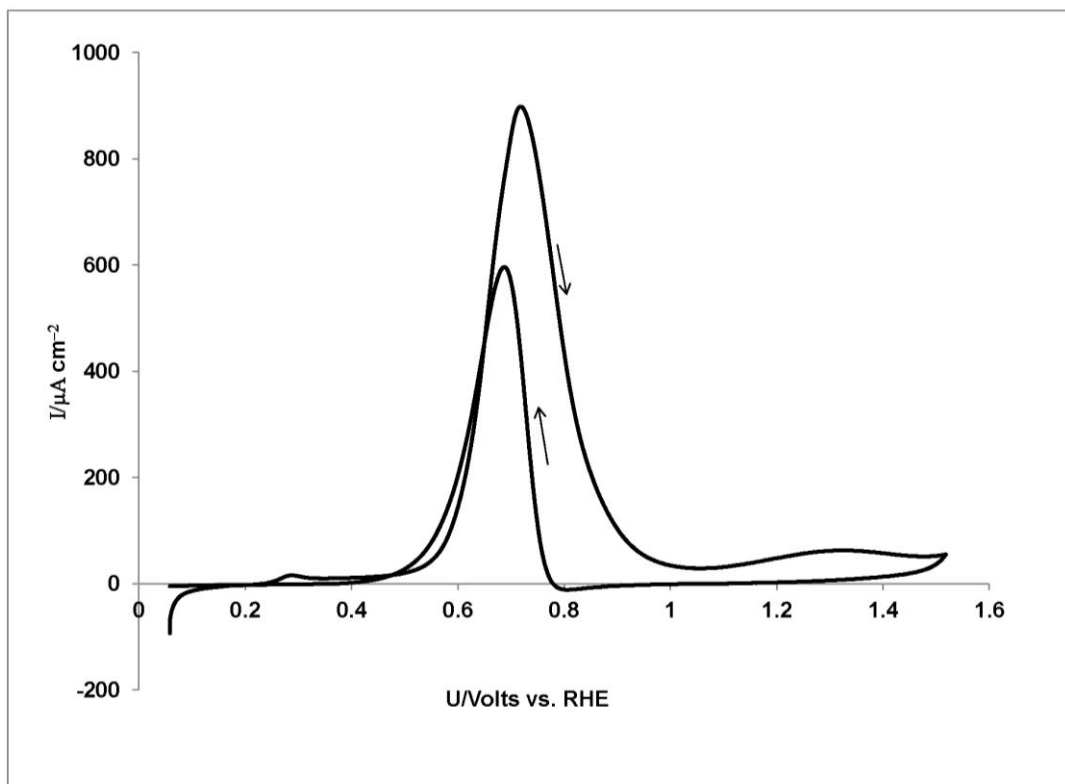


Figure 1. CV scan for methanol oxidation at a Pt electrode in 1 M HClO₄ containing 0.005 M methanol. The electrode was pre-treated and then reduced at 0.06 V before scanning at 5 mV/sec.

3.2 Anodic Charge by Chronocoulometry

After pre-treatment, the potential was pulsed to 0.4 V and the resulting anodic charge, Q_a , was recorded starting at 0.1 s. Plots of Q_a versus time for 0.001 and 0.005 M methanol appear in figure 2a and b, respectively. As there is no desorption of material (see section 3.1), Q_a corresponds to the accumulation on the surface of partially oxidized methanol.

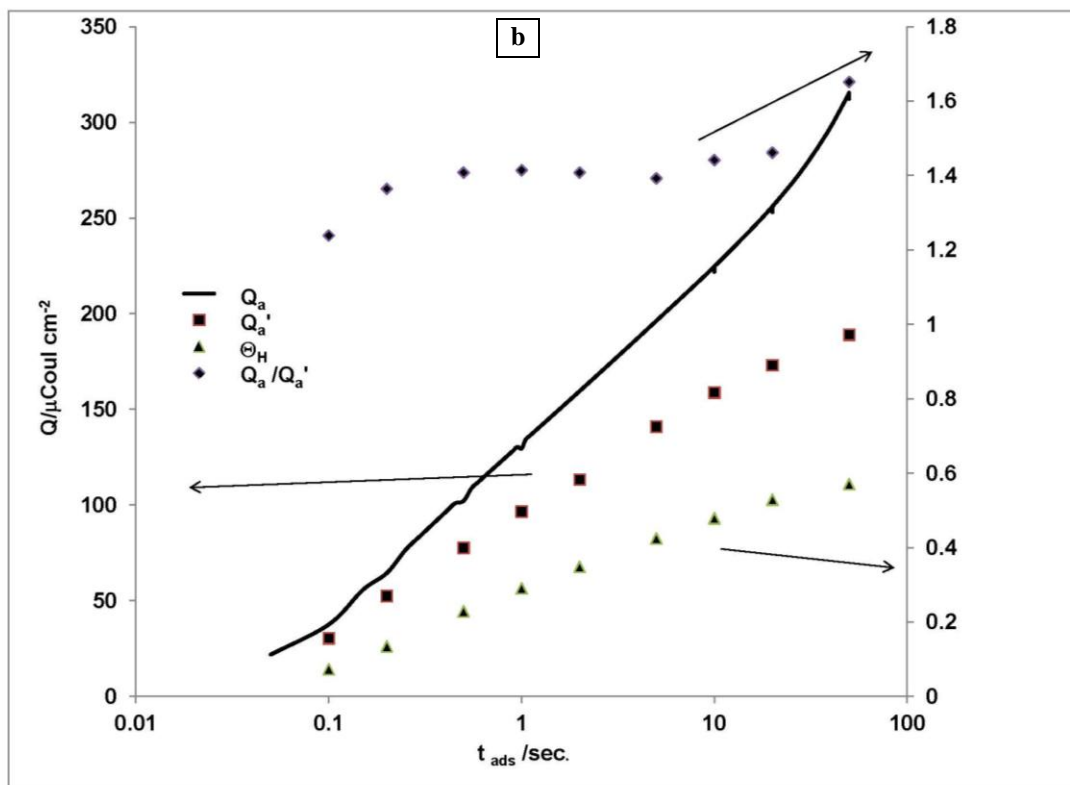
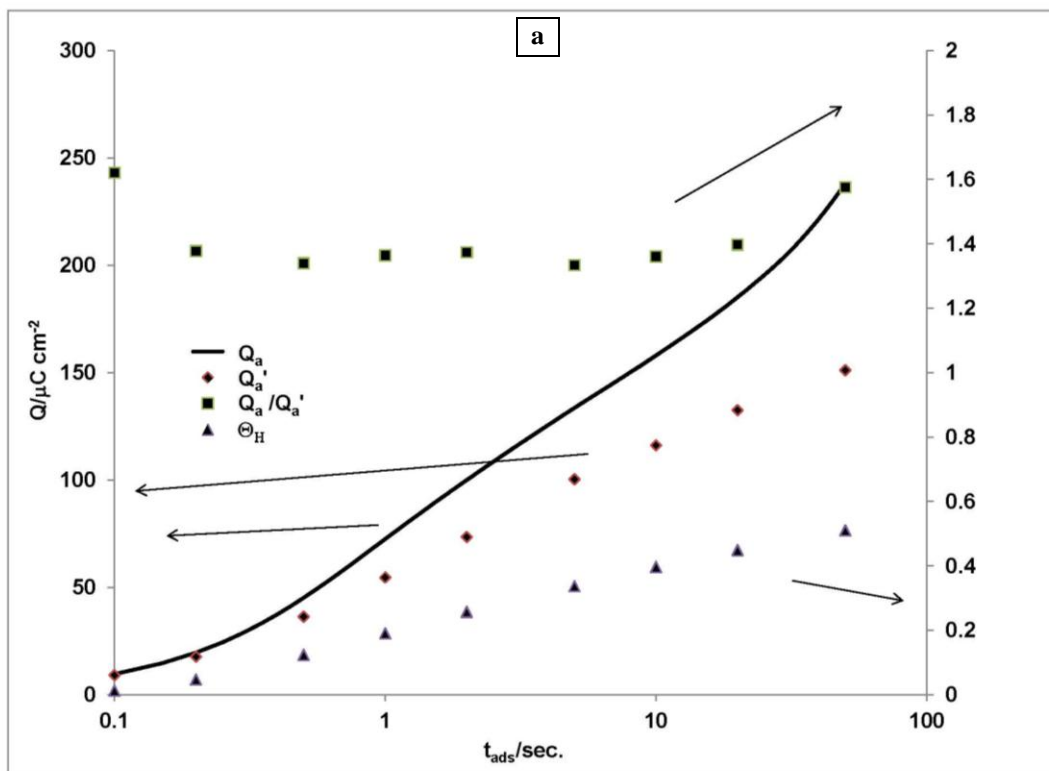


Figure 2. Values of charge corresponding to methanol adsorption: (a) at 0.4 V from a 0.001 M solution and (b) at 0.3 V from a 0.005 M solution of methanol. Q_a = charge measured during adsorption. Q_a' = charge measured during linear anodic scan of adlayer. Θ_H = fractional surface coverage based on the hydrogen underpotential deposition (UPD).

3.3 Anodic Charge by Linear Anodic Scan

Under the same conditions as in section 3.2, the accumulation of material on the electrode at 0.4 V was sampled by applying a linear anodic scan of 200 V/s. Sample traces appear in figure 3. The traces obtained for the 1 M HClO₄ supporting electrolyte were identical over the full range of adsorption times. Values of Q_a' were obtained by integration of the closed areas between the traces (with time as the x -axis) for the supporting electrolyte and those for different values of $t_{(ads)}$. The calculated values of Q_a' are plotted in figures 2a and b Q_a' is the charge corresponding to the oxidation to CO₂ of the material adsorbed on the electrode surface if the following conditions are met: (1) no desorption of oxidation intermediates occurs during the scan and (2) all adsorbed material is oxidized by the time the scans for the supporting electrolyte and the methanolic solution merge at high potentials. Good adherence to calculated diffusion rates for related adsorbates (32, 33) suggests that the latter conditions are likely met here.

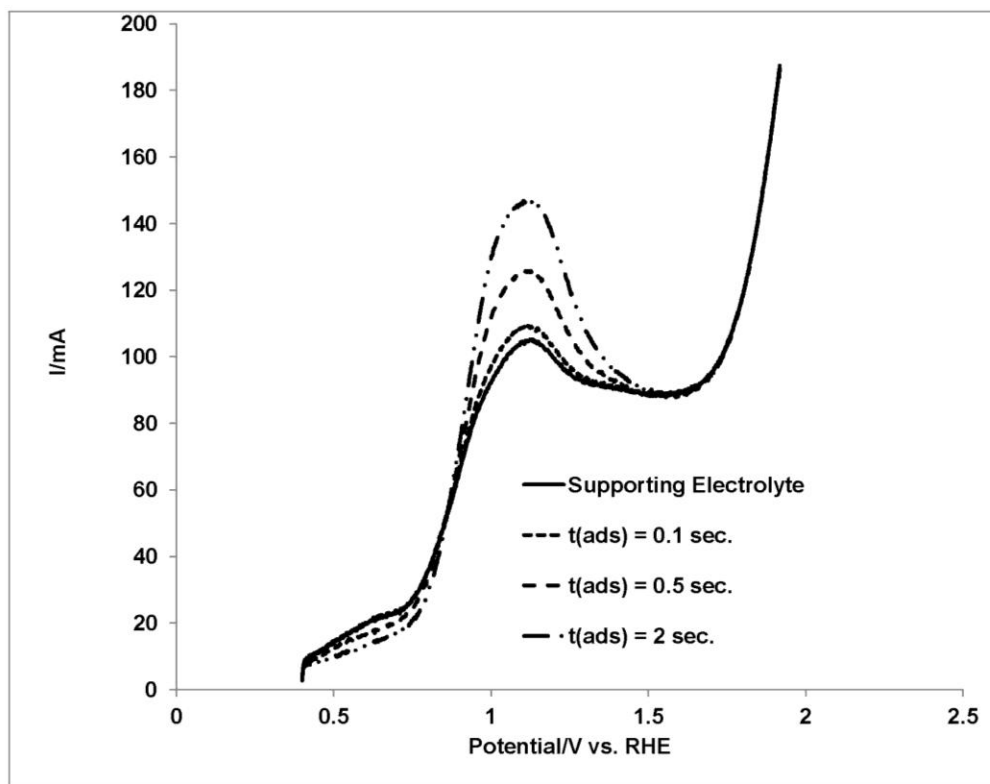


Figure 3. Representative anodic CV scans at 200 V/s for tracking (by oxidation) the adsorption of methanol at 0.4 V from a 0.001 M solution of methanol in a 1 M HClO₄ supporting electrolyte.

3.4 Measurement of Fractional Surface Coverage by Hydrogen Underpotential Deposition

The approach used here is similar to that appearing in a previous publication (34). After each pre-treatment sequence, the potential was stepped to 0.4 V for 10 ms to allow for rapid reduction of the surface before stepping to the particular potential of interest. A linear cathodic potential

scan at 200 V/s was then applied to obtain the charge corresponding to hydrogen UPD, Q_H , which could be accommodated on the surface partially covered by the methanolic adsorbate. Representative traces for such scans appear in figure 4. Values of, Q_H were determined by integration of the area (with adsorption time as the x axis) under the trace from 0.4 V to the inflection point (corresponding to molecular hydrogen evolution) appearing at the most negative t potentials. As only differences in Q_H are employed in the analyses below, changes in the double-layer capacity are assumed to have only a small effect. Based on the blockage of hydrogen adsorption sites, the fractional coverage of the surface, Θ , with methanol is

$$\Theta_M = ({}^S Q_H - Q_H) / {}^S Q_H, \quad (1)$$

where ${}^S Q_H$ is the “saturation coverage” with hydrogen of the bare surface. Values of Θ_M are plotted on figures 2a and b and used in figure 5 and in all subsequent figures.

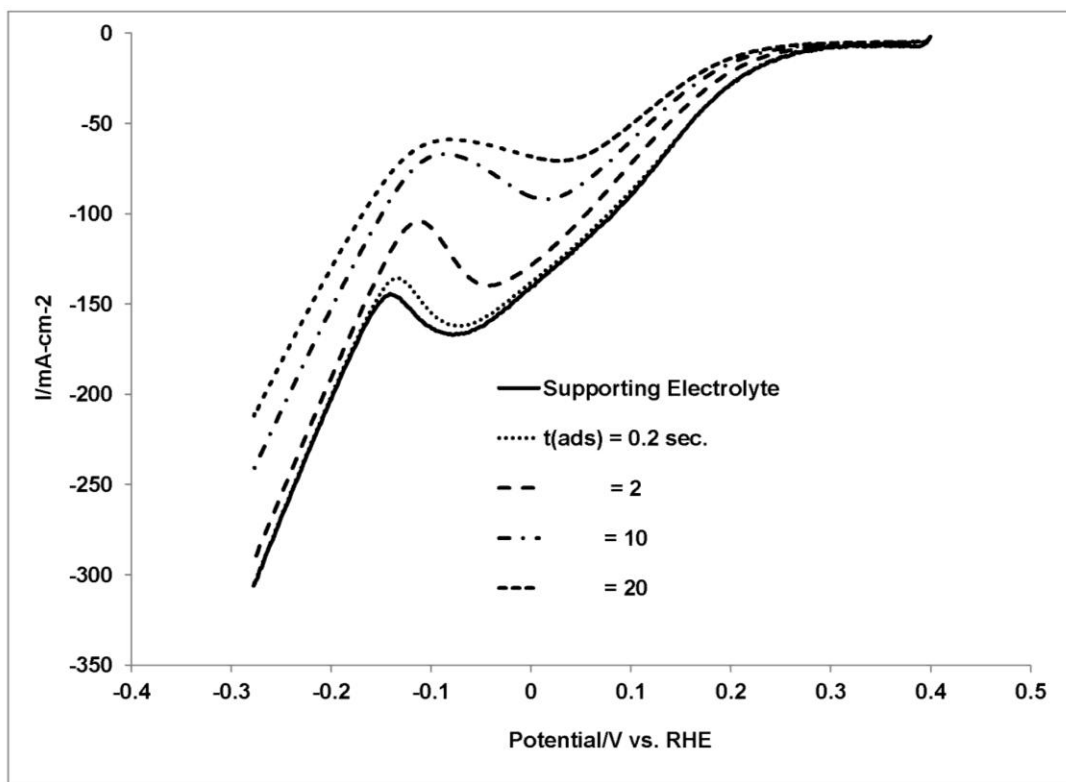


Figure 4. Representative cathodic CV scans at 200 V/s for tracking (by hydrogen UPD) the adsorption of methanol from a 0.001 M solution of methanol in a 1 M HClO_4 supporting electrolyte.

3.5 Comparison of Q_a with Q_a'

As discussed above, Q_a is the charge passed when methanol is adsorbed and Q_a' is the charge corresponding to further oxidation/desorption of the resulting adlayer. At 0.4 V, no desorption of adsorption/oxidation products to the electrolyte is expected (see section 3.1). From figures 2a and b, the ratio $Q_a/Q_a' = \sim 1.4$ for most of the range of surface coverages encountered and for the

two concentrations explored at 0.4 V. Most of the spectroscopic evidence (18, 19, 21, 24, 27) suggests that the methanolic adlayer consists of variously bonded species with the stoichiometry CHO and CO. For CO only, (4e oxidation to CO and 2e oxidation to CO₂), the expected ratio Q_a/Q_a' would be 2.0. For CHO (only 3e oxidation to CHO and 3e oxidation to CO₂), the expected ratio Q_a/Q_a' would be 1.0. For a mixture of the two stoichiometries, the ratio Q_a/Q_a' would be given by equation 2:

$$Q_a/Q_a' = (4 P + 3)/(3-P), \quad (2)$$

where P = percentage of the adlayer having the CO stoichiometry. For $Q_a/Q_a' = 1.4$, the CHO and CO stoichiometries would be present in equal amounts. Similar results were obtained by Wilhelm et al (26). However, there is also evidence for a CH₂O stoichiometry (24), which would have a downward effect on Q_a/Q_a' .

3.6 Comparison of Q_a' with ΔQ_H

As discussed in section 3.5, Q_a' is the charge corresponding to oxidation of the adlayer to CO₂. $\Delta Q_H = Q_H^s - Q_H$ corresponds to the hydrogen adsorption sites blocked by the methanolic adlayer. The ratio, $Q_a' / \Delta Q_H = R$ represents the average number of electrons per hydrogen site for the oxidation of the methanolic adlayer. Plots of Q_a' , ΔQ_H , and R for 0.4 V, 0.001 M methanol and 0.3 V, 0.005 M methanol, appear in figures 5a and b, respectively. For both potentials and concentrations, R drops from an initial value of ~2 to a final value of ~1.2. This is similar to results reported by Leiva et al. (10) for a sulfuric-acid-supporting electrolyte and was ascribed to the presence of mainly bridged CO (linear or “atop” CO would result in R=2). However, considering all of the possible hydrogen-containing fragments and bondings, the R values can probably only be used to further indicate the complexity of the adlayer and provide motivation for investigating hydrogen blocking as the method for following the kinetics of the adsorption process. Values of R between 1.1 and 1.2 have also been reported by a number of investigators (1) for a wide range of methanol concentrations, electrode activations, and supporting electrolytes.

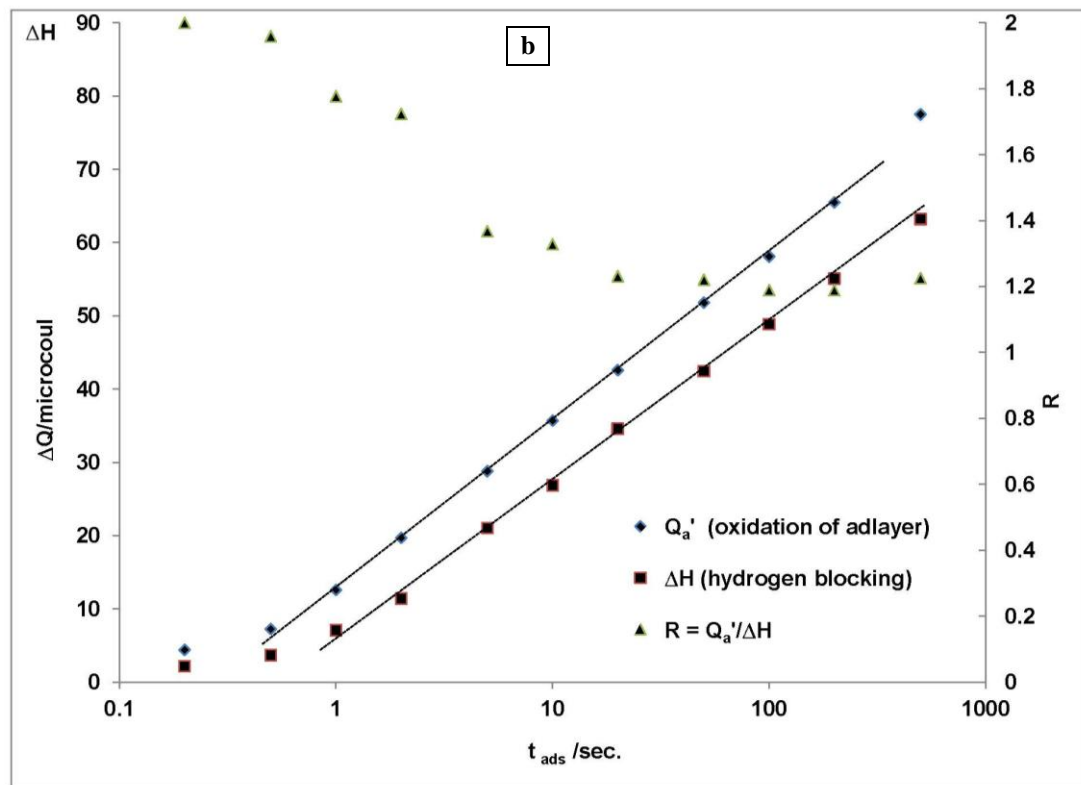
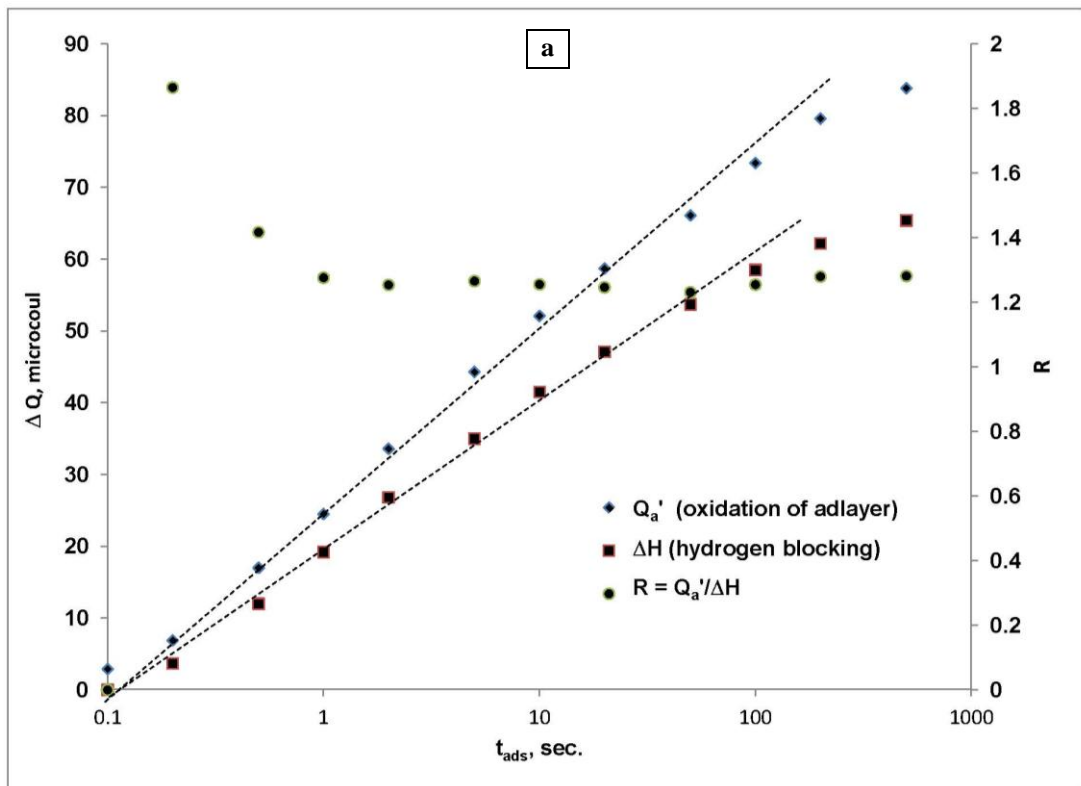


Figure 5. Values of charge corresponding to oxidation of the methanolic adlayer and blocking of hydrogen adsorption sites at (a) 0.4 V, 0.001 M methanol and (b) 0.3 V, 0.005 M methanol.

3.7 Kinetics of Methanol Adsorption Measured by Hydrogen Blocking

The results appearing in figures 6a and b were obtained using the procedure discussed in section 3.4. For both concentrations of methanol, the time dependence of fractional surface coverage for adsorption potentials from 0.1 to 0.5 V follow the parallel dashed lines in the figures and suggests adherence to the Elovich (or Roginsky-Zeldovich) equation (35) for adsorption on a heterogeneous surface:

$$d\Theta_M / dt_{ads} = kC e^{-m\Theta}, \quad (3)$$

where C is the concentration of adsorbate and k and m are constants.

In integrated form,

$$\Theta_M = A \ln C + \ln t_{ads}/m, \quad (4)$$

where A is a lumped constant.

The semi-logarithmic relationships of figures 6a and b hold for fractional coverages below 0.1 to 0.5 or higher. Where the linear relationship holds,

$$d\Theta_M / dt_{ads} = S / t_{ads}, \quad (5)$$

where S is the slope of the parallel lines of figures 6a and b and has the value $0.09 t_{ads}$ monolayer.

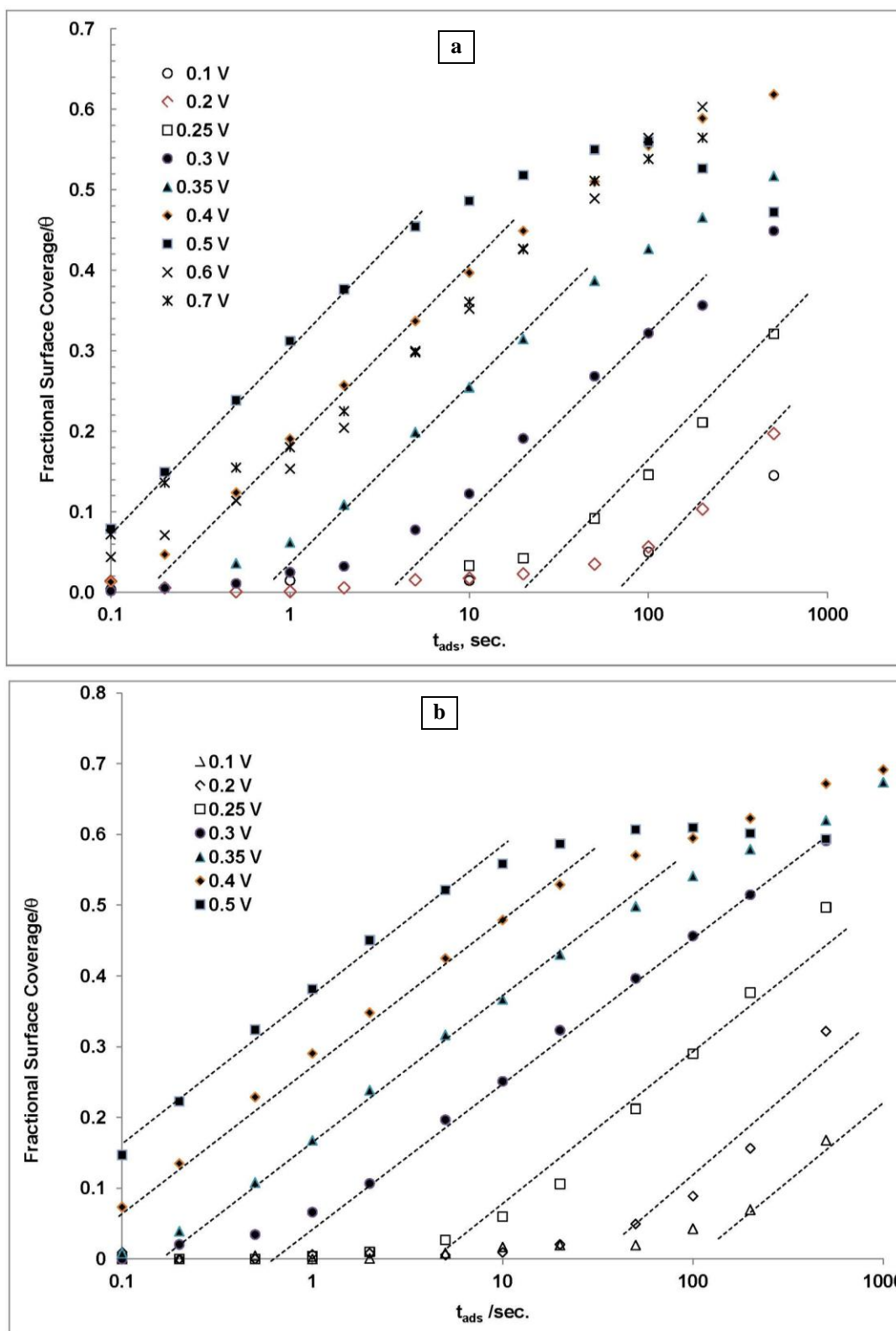


Figure 6. Fractional surface coverage of electrode with methanol as determined by hydrogen blocking. Methanol adsorbed from (a) a 0.001 M solution of methanol and (b) a 0.005 M solution of methanol.

Given the irreversible nature of the adsorption, the plateau values of Θ do not have thermodynamic significance, but represent steric limitation; higher values can be anticipated for extended periods of time. As is shown below, the spacing between the parallel dashed lines suggest the existence of a Tafel relationship when a comparison is made between the rates of adsorption at different potentials for fixed values of Θ_M . It can be seen that rates diminish for potentials above 0.5 V in figure 6a. This coincides with the observation of production and desorption of soluble oxidation products as mentioned in section 3.1.

Bagotzky and Vassiliev (2) were first to recognize that the Elovich equation can be applied to the adsorption of methanol and other small organic molecules. Their study was performed using sulfuric acid as the supporting electrolyte. Their reported rates were significantly lower than those reported here. Specifically, in figure 6 of that paper, at 0.4 V and at a concentration of 0.005 M methanol, half the plateau value is reached in approximately 20 s, versus 2 s in this study. The difference is likely due to the effect of specifically adsorbed sulfate ion as is discussed in a section below.

3.8 Dependence of Adsorption Rate on Methanol Concentration

Θ_M versus log time data similar to that of figures 6a and b was obtained at 0.4 V and a range of methanol concentrations. Rates of adsorption at $\Theta_M = 0.5$ were taken from the plots and the results were plotted against the methanol concentration in figure 7 to test the concentration dependence predicted by equation 3. The trendline in figure 7 shows that the anticipated linear relationship between adsorption rate and concentration is good.

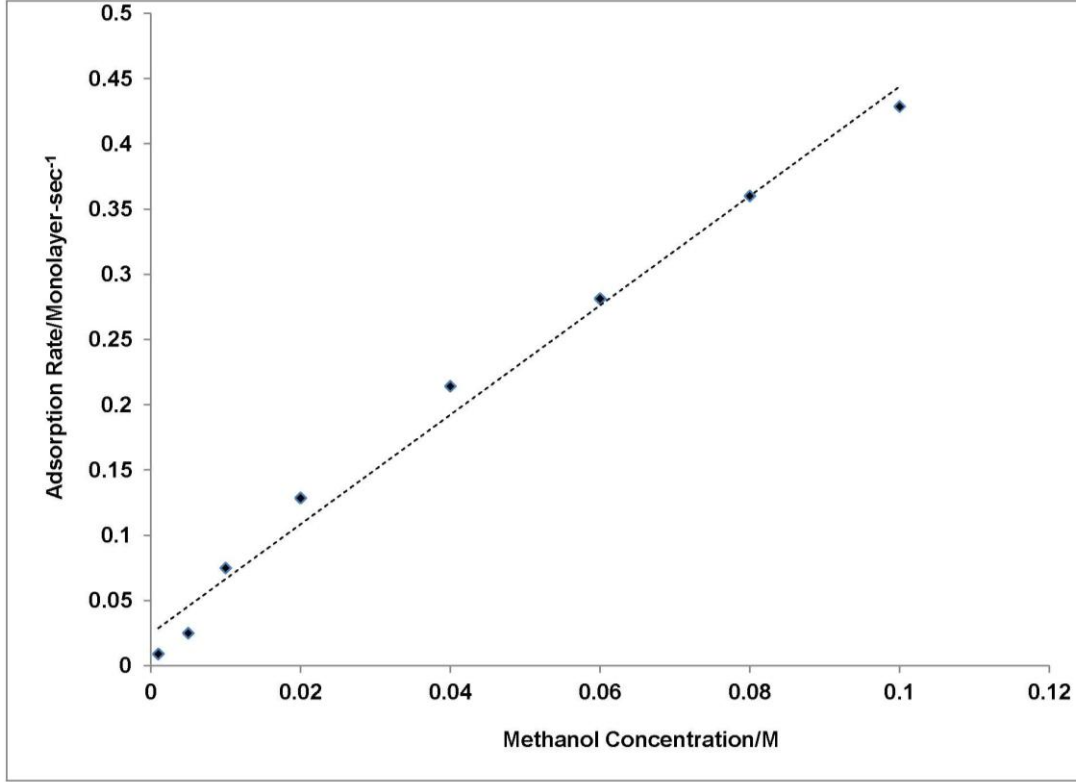


Figure 7. Dependence of adsorption rate on methanol concentration. Adsorption rates were measured at 0.4 V and a fractional surface coverage of 0.5.

3.9 Dependence of Adsorption Rate on Electrode Potential

For an irreversible anodic reaction, the Tafel Equation can be written as (36)

$$U - U_0 = a - b \log i \quad (6)$$

$$b \text{ is the Tafel slope} = 2.303 RT/\alpha nF, \quad (7)$$

where α = symmetry (transfer) coefficient

n = number of electrons in the rate-determining step

U = electrode potential vs. the reference electrode

F , R & T have their usual meanings.

Figure 8 applies equation 7 to the experimental $\Theta_M - t_{ads}$ data obtained through hydrogen-blocking experiments. For this purpose, the values of Θ_M appearing in figures 6a and b were converted to ΔQ_H by multiplying by sQ_H and re-plotting. Rates of adsorption as virtual current, I_{ads} , were obtained from the slopes of the linear sections of the plots, at points corresponding to $\Theta_M = 0.2$. The resulting values of I_{ads} versus U are plotted in figure 8. As the linear sections of the Θ_M and corresponding ΔQ_H vs. $\log t_{ads}$ plots are parallel, points corresponding to any other

value of Θ_M in the linear regions of those plots would yield the same slopes for the of I_{ads} versus U plots. The dashed line in figure 8 is the computer-generated trendline for the 0.005 M methanol points. The points for the 0.001 M methanol are (with the exception of the 0.5-V result) parallel to those for the higher concentration in accordance with the concentration dependence discussed in section 3.8. The trendline has a Tafel slope of 80 mV, which corresponds to $\alpha n = 0.8$. This could be interpreted as corresponding to a 2-electron dehydrogenation process (to an HCOH stoichiometry) if $\alpha = 0.4$. The particularly high value of I_{ads} at 0.5 V for the lower methanol concentration may be due to incipient “turnover” current. Figure 9 presents values of hydrogen surface coverage, Θ_H , for the methanol-free surface obtained by integrating the charge measured during a slow anodic scan. A comparison of figures 8 and 9 leads to the conclusion that the Tafel relationship holds from $\Theta_H = 0.44$ (at 0.1 V) to 0 (above 0.4 V). Hence, the suggestion (1, 2) that methanol coverage declines at low potentials due to blockage by adsorbed hydrogen may be true only for $\Theta_H > 0.4$, the effect being steric in nature. Potentials lower than 0.1 V were not explored here because the molecular hydrogen generated interferes with the accurate measurement of ΔQ_H and the higher adsorption times tend to fall outside of the retention of surface purity as measured in the supporting electrolyte. A Tafel slope of 120 mV was reported by Herrero et al. (8) through analysis of the early transient current obtained on stepping from a low (methanol-free) potential for 110- and 100-oriented single crystals of Pt. That result probably applied to $\Theta_M \sim 0$.

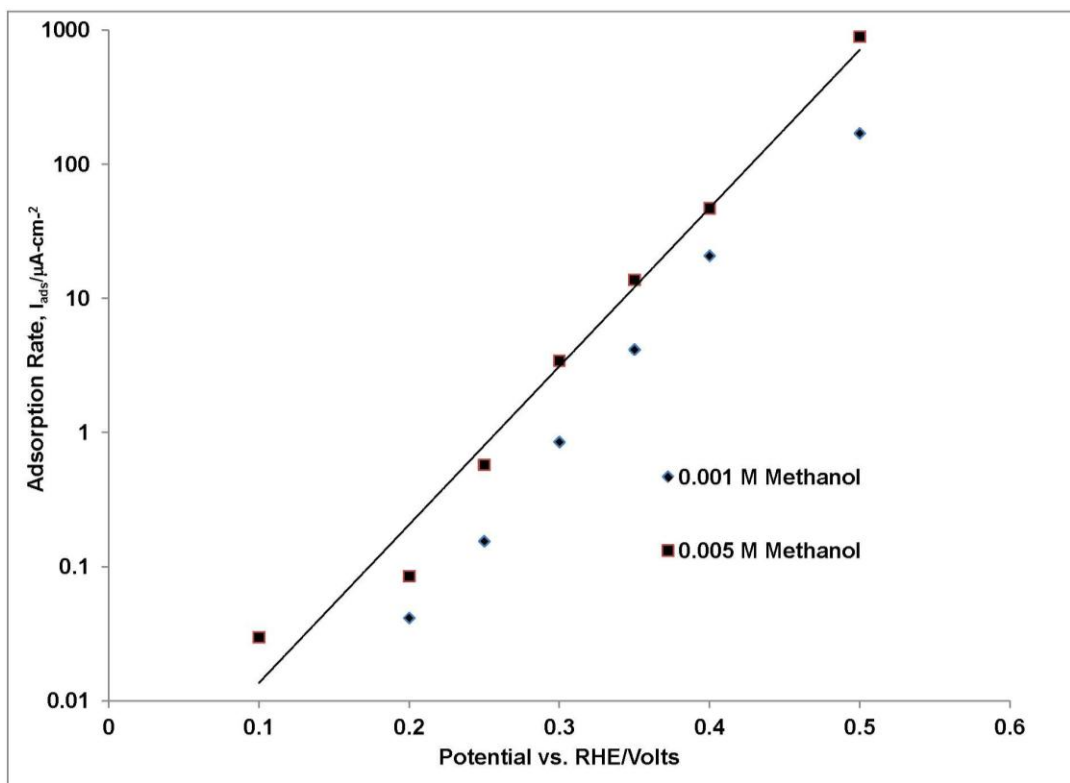


Figure 8. Potential dependence of the methanol adsorption rate.

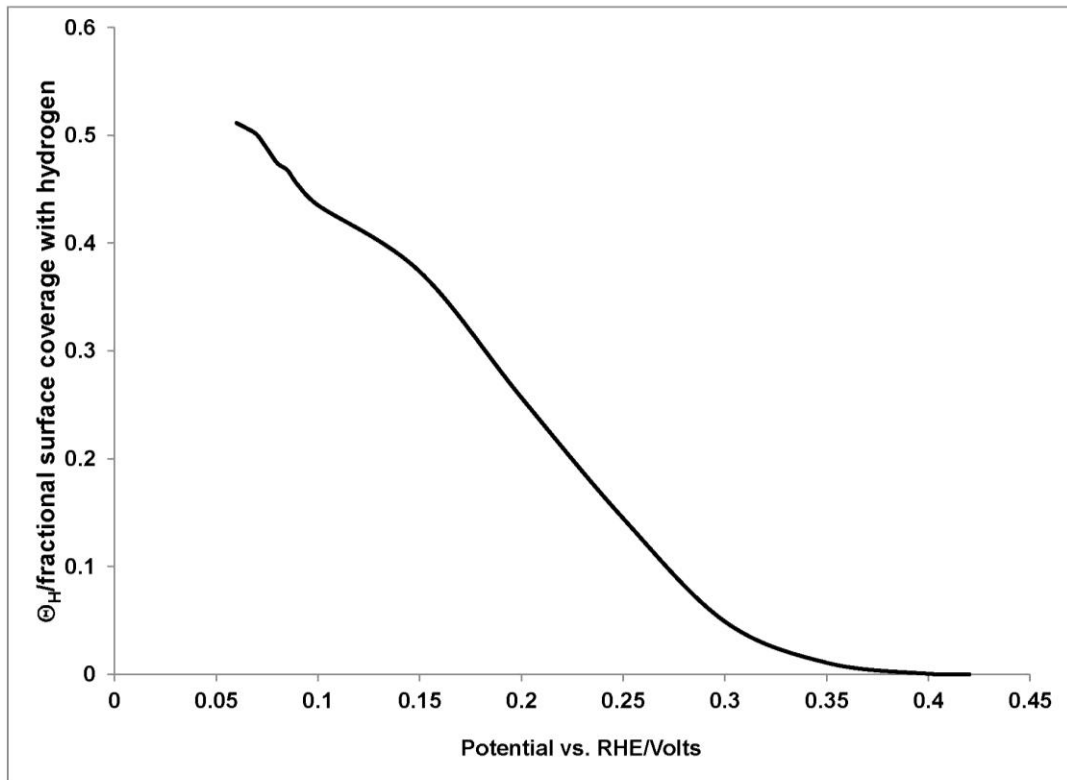


Figure 9. Fractional surface coverage of methanol-free electrode with hydrogen.

3.10 “Poisoning Effect” of Adsorbed Methanol

As mentioned in section 1, the methanolic adlayer has been shown to contain species with a number of stoichiometries and modes of attachment to the surface. The purpose of this section of the present study was to examine how Θ_M affects the current that flows at the low end of anodic overvoltage that is most relevant to the fuel cell application. The electrode potential, 0.6 V was chosen for examination because it is possible to make a good differentiation at that potential between the fractions of the total current I_{total} that lead to surface accumulation only (I_{ads}) and to oxidation to products that are desorbed and released to the solution (I_{ox}). Figure 10 shows the partial currents obtained as follows:

1. After the usual activation steps, the electrode was reduced at 0.4 V for 0.1 s and stepped to 0.6 V, and I_{total} was recorded.
2. The Θ_M versus $\log t_{ads}$ plot of figure 6a was converted to the corresponding current using equation 5. That current, which corresponds to hydrogen site occupancy, was converted to the virtual oxidation/adsorption current, I_{ads} , by multiplying by the product of plateau ratio's of figures 2a and 5a (1.4 and 1.22, respectively).
3. I_{ox} , was obtained by subtracting I_{ads} from I_{total} .

In figure 11, the calculated values of I_{ox} are plotted against the Θ_M values taken from figure 6a. The computer-generated trendline tends to confirm in that I_{ox} decreases only linearly with increased occupancy of the surface with adsorbed methanolic species. It may be noted that this result could not be significantly influence by errors in the assumptions leading to the I_{ads} values as the latter amount to a relatively small contribution to the calculated values of I_{ox} .

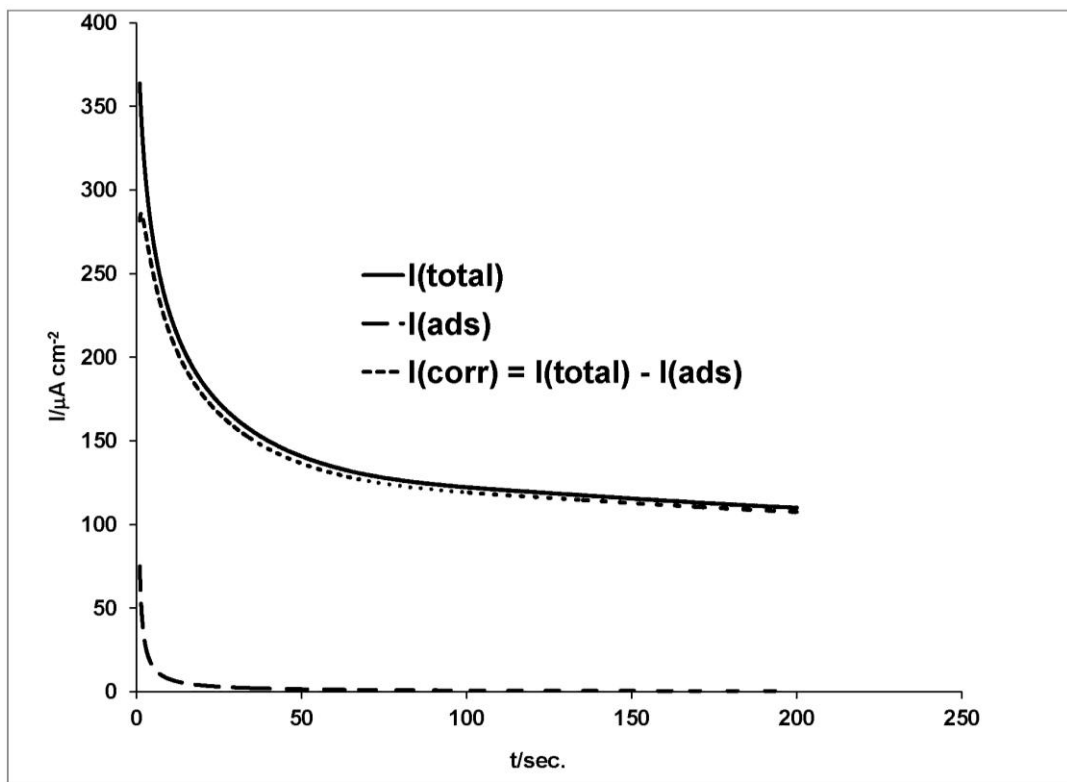


Figure 10. Partial currents at 0.6 V.

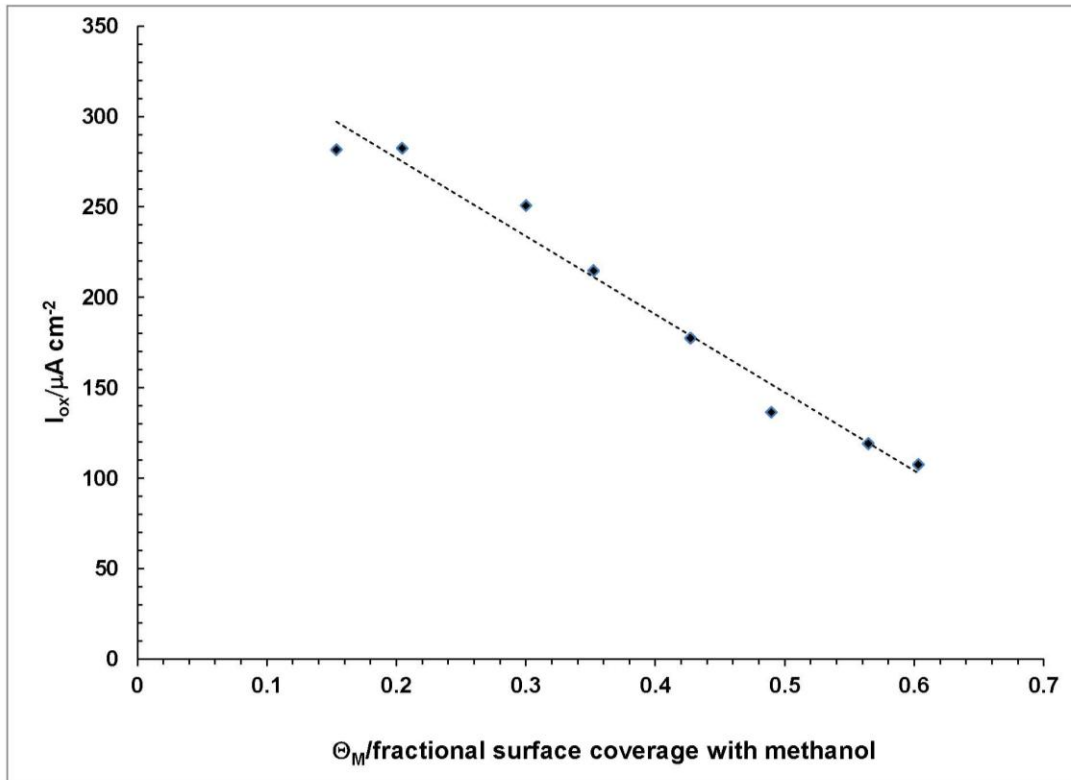


Figure 11. Dependence of oxidation/desorption current on methanolic surface coverage.

3.11 Effect of Adsorbed Anions on the Adsorption and Oxidation of Methanol

The negative effect of adsorbable anions, including bisulfate and chloride ions on the anodic oxidation of methanol on Pt electrodes is well known (2, 4, 9, 15, 37). For platinized Pt electrodes, Horanyi and Vertes (15) using a $^{36}Cl^-$ radiotracer showed that the methanol displaced specifically adsorbed chloride ions in a perchloric acid electrolyte. In a 0.5 M sulfuric acid electrolyte at 0.5 V, Sobkowsky and Wiekowski (16) showed that added chloride ions decreased the rate of adsorption of methanol on a platinized Pt electrode. The purpose of this part of the present investigation was to obtain preliminary information on the effect on adsorption of the more strongly adsorbed chloride ion and the relatively weakly adsorbed sulfate ion on methanol adsorption/oxidation under the same conditions as in the other sections of this report. The polarization curves of figure 12 were obtained by applying an anodic scan of 5 mV/s to the electrode after activation and reduction at 0.4 V. The supporting electrolyte was 1 M $HClO_4$ for all three traces. At this slow sweep speed, the currents correspond mainly to methanol “turnover,” the currents due to adsorption/surface accumulation of methanol being negligible. From the figure it can be seen that the addition of sulfuric acid mainly reduces the peak oxidation current, whereas the addition of hydrochloric acid virtually eliminates the oxidation of methanol at low potentials.

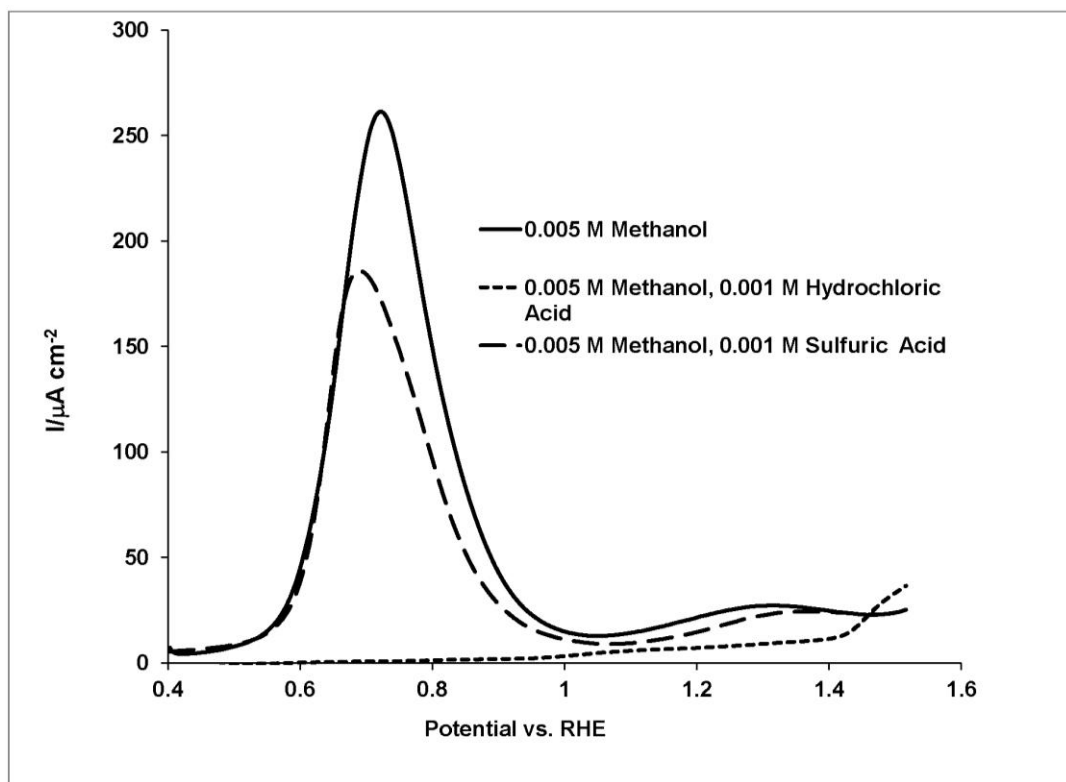


Figure 12. Effect of specifically adsorbed anions on anodic oxidation of methanol.

The adsorption of methanol in the presence of chloride and sulfate ions was followed using the same procedure as in section 3.4: after activation, the potential was stepped to 0.4 V to allow for adsorption of both methanol and the anions. Under those conditions, the starting fractional surface coverage (based on hydrogen adsorption sites) of chloride ions would be at the equilibrium values of 0.3 (38). The starting coverage with sulfate ions would be approximately 0.05 based on the results reported by Dalbeck and Vielstich (39). Application of a linear cathodic scan at 200 V/s, allows one to determine Θ_M as in section 3.4 without interference by the adsorbed anions, as the latter are completely desorbed during the scan and do not affect the measured values of Q_H (4, 40). Figure 13 compares the time dependence of Θ_M under the described conditions. It can be seen that adsorbed chloride ions cause a decrease in the rate of methanol adsorption of approximately three orders of magnitude, paralleling the extreme decrease in anodic oxidation current apparent in figure 12. As the coverage with Cl^- is far from complete, this implies more than a simple steric effect on the initial dissociation/adsorption of methanol. This also exceeds the one order of magnitude decrease in adsorption rate that would be expected if the effect of the adsorbed Cl^- were simply to occupy the sites with the highest heats of adsorption, similar to adsorbed methanol itself. The concurrent extreme effect of Cl^- adsorption on the polarization curve (i.e., on I_{ox}) suggests that both processes are dependent on the same initial dehydrogenation step. This contrasts sharply with the competitive adsorption of CO and Cl^- (40), which involves no dissociation in the adsorption of the organic molecule. The

adsorption of CO is diffusion-controlled both in the absence and presence of Cl^- , readily displacing the anion from the surface. On the other hand, the adsorption of ethane, which does involve initial dehydrogenation, is noticeably affected by Cl^- (41) but to a lesser extent than is methanol adsorption. The effect of sulfate ions on Θ_M is much less pronounced and the effect is largely gone at $t_{\text{ads}} > 100$ s. This parallels the slight effect that sulfate ions have on the anodic oxidation of methanol as seen in figure 12 (below the peak current).

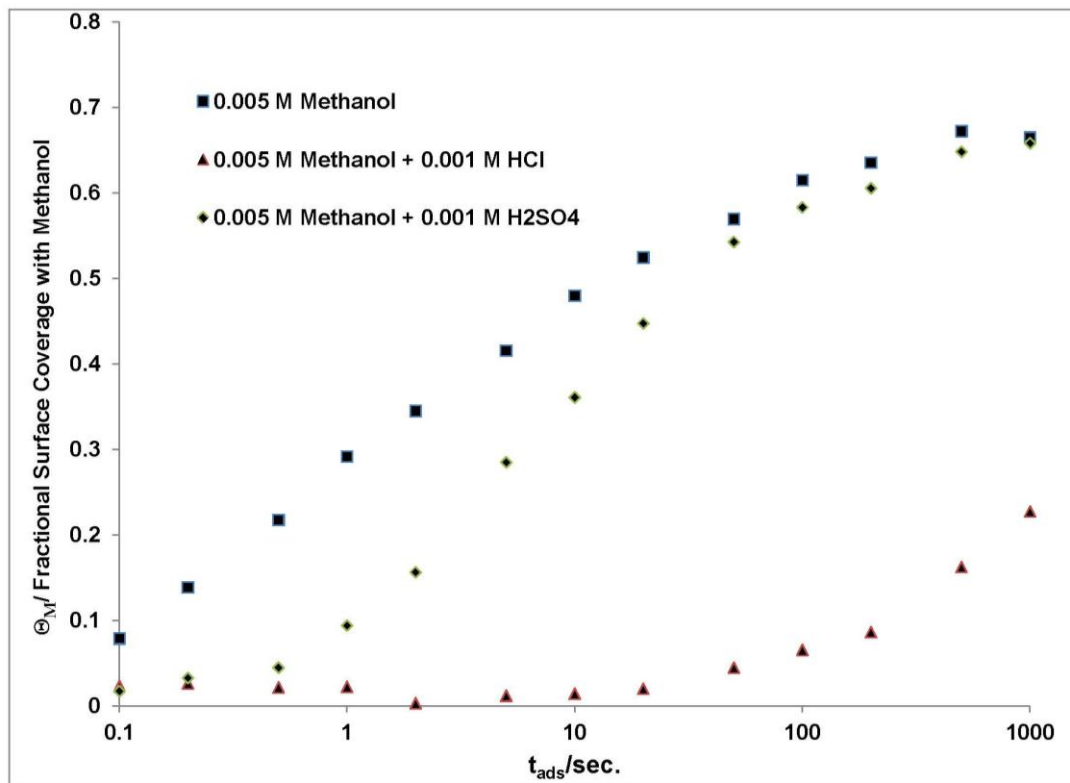


Figure 13. Effect of specifically adsorbed anions on the methanol adsorption rate.

4. Conclusion

The use of a “staircase” of potentials provides a highly reproducible surface state on a Pt electrode, allowing detailed analysis of the kinetics of adsorption of organic substances. For methanol, adsorption is best monitored by the blocking effect on hydrogen UPD. Below ~ 0.5 V versus a reference RHE, adsorption of methanol occurs with only the accumulation of partially oxidized methanolic species. Above that potential, more complete oxidation of methanol leads to desorbed final products of oxidation. Therefore, the adsorption processes can be studied in detail in the lower potential range. In that range of potentials, the rate of methanol adsorption was found to follow classical laws for an electrochemical oxidation process (i.e., Tafel relationship), which is also dependent on the extent of occupancy of heterogeneous surface sites (i.e., Elovich

equation). Adsorbed methanol has a linear “poisoning effect” on the anodic current that produces final products at potentials higher than ~ 0.5 V. Adsorbed chloride ions drastically reduce both the adsorption of methanol and the anodic current. The effect of bisulfate ions is only moderate by comparison.

5. References

1. Parsons, R.; Vandernoot, T. *J. Electroanal. Chem.* **1998**, *257*, 9–45.
2. Handbook of Fuel Cells, vol. 2, chapter 41 by T. Iwasita, pub. By John Wiley & Sons, Ltd, edited by W. Vielstich, A. Lamm and H Gasteiger, 2003.
3. Wasmus, S.; Kuver, A. *J. Electroanal. Chem* **1999**, *461*, 14–31.
4. Bagotzky, V. S; Vassilyev, Yu. B.; Weber, J.; Pirtskhalava J. N. *J Electroanal. Chem.* **1970**, *27*, 31–46.
5. Bagotzky, V. S.; Vassiliev, Yu. B. *Electrochim. Acta* **1966**, *11*, 1439–1461.
6. Bagotzky, V. S.; Vassiliev, Yu. B.; Khazova O. A. *J. Electroanal. Chem.* **1977**, *81*, 229–238.
7. Gasteiger, H. A.; Markovic, N.; Ross, Jr., P. N.; Cairns, E. J. *J. Electrochem. Soc.* **1994**, *141*, 1795–1803.
8. Herrero, E.; Franaszczuk, K.; Wieckowski, A. *J. Phys Chem.* **1994**, *98*, 5074–5083.
9. Kamath, V. N.; Lal, H. *J. Electroanal. Chem.* **1970**, *24*, 125–135.
10. Leiva, E.P.M.; Giordano, M. C. *J. Electroanal. Chem.* **1983**, *158*, 115–130.
11. Wilhelm, S.; Iwasita, T.; Vielstich, W. *Electroanal. Chem.* **1987**, *238*, 383–391.
12. Xu, W.; Lu, T.; Liu, C.; Xing, W. *J. Phys Chem. B* **2006**, *110*, 4802–4807.
13. Hao, E.; Scott, Yu, K.; Reeve, R. W. *J. of Electroanal. Chem.* **2003**, *547*, 17–24.
14. Leiva, E.P.M.; Giodano, M. C. *J. Electroanal. Chem.* **1983**, *158*, 115–130.
15. Horanyi, G.; Vertes, G. *Electroanal. Chem. and Interfacial Electrochem.* **1974**, *51*, 417–423.
16. Sobkowski, J.; Wieckowski, A. J. *Electroanal. Chem. and Interfacial Electrochem.* **1973**, *41*, 373–379.
17. Podlovchenko, I.; Kazarinov, V. E.; Stenin, V. F. *Soviet Electrochem.* **1970**, *6*, 241–252.
18. Beden, B.; Lamy, C.; Bewick, A.; Kunimatsu, K. *J. Electroanal. Chem.* **1981**, *121* 343–347.
19. Beden, B.; Juanto, S.; Leger, J. M.; Lamy, C. *J. Electroanal. Chem.* **1987**, *238*, 323–331.
20. Gasteiger, H. A.; Ross Jr., P. N.; Cairns, E. J. *Surf. Sc.* **1993**, *293*, 87–80.

21. Kunimatsu, K. *J. of Electron Spectroscopy and Related Phenomena* **1983**, 30, 215–220.
22. Legar, J. M. *J. Appl. Electrochem.* **2001**, 31, 767–771.
23. Xia, X. H.; Iwasita, T.; Ge, F.; Vielstich, W. *Electrochim. Acta* **1996**, 41, 711–718.
24. Iwasita, T.; Nart, F. C. *J. Electroanal. Chem.* **1991**, 317, 291–298.
25. Juanto, S.; Beden, B.; Hahn, F.; Legar, J. M.; Lamy, C. *J. Electroanal. Chem.* **1987**, 237, 119–129.
26. Wang, H.; Löffler, T.; Baltruschat, H. *J. Appl. Electrochem.* **2001**, 31, 759–765.
27. Wilhelm, S.; Iwasita, T.; Vielstich, W. *J. Electroanal. Chem.* **1987**, 238, 383–391.
28. Iwasita, T.; Vielstich, W. *J. Electroanal. Chem.* **1986**, 201, 403–408.
29. Herrero, E.; Franaszczuk, K.; Wieckowski, A. *J. Phys. Chem.* **1994**, 98, 5074–5083.
30. Tripkovic, A. V.; Popvic, K. D.; Momcilovic, J. D.; Drazic, D. M. *Electrochimica Acta* **1998**, 44, 1135–1145.
31. Gilman, S. *Electrochimica Acta* **2012**, 65, 141–148.
32. Gilman, S. *J. Electroanal. Chem.* **2013**, 692, 53–59.
33. Gilman, S. *J. Phys. Chem.* **1963**, 67, 78–84.
34. Gilman, S. *J. Power Sources* **2012**, 197, 65–71.
35. *Physical Chemistry of Surfaces*, 3rd edition, John Wiley and Sons Inc., New York, 1976, p. 650.
36. *Analytical Electrochemistry*, third edition by Joseph Wang, John Wiley and Sons, 2006 p. 15.
37. *Electrochemical Processes in Fuel Cells* by M. W. Breiter, Springer-Verlag, 1965.
38. Gilman, S. *J. Phys. Chem.* **1964**, 68, 2099–2111.
39. Dalbeck, R.; Vielstich, W. *Electrochim. Acta* **1995**, 40, 2687–2688.
40. Gilman, S. *J. Phys. Chem.* **1964**, 68, 2112–2119.
41. Gilman, S. *J. Phys. Chem.* **1967**, 71, 2424–2433.

1 DEFENSE TECHNICAL
(PDF) INFORMATION CTR
DTIC OCA

2 DIRECTOR
(PDFS) US ARMY RESEARCH LAB
IMAL HRA MAIL & RECORDS MGMT
RDRL CIO LL TECH LIBRARY

6 US ARMY RSRCH LAB
(PDFS) RDRL SED E J SHAFFER
RDRL SED C
C LUNDGREN
D CHU
R JIANG
W BEHL
J READ

1 CERDEC HDQ
(PDF) ATTN EDWARD PLICHTA

INTENTIONALLY LEFT BLANK.